STAT5-mediated chromatin interactions in superenhancers activate IL-2 highly inducible genes: Functional dissection of the *Il2ra* gene locus

Peng Li[a,1,2], Suman Mitra[a,1,3], Rosanne Spolski[a,1], Jangsuk Oh[a,1], Wei Liao[a], Zhonghui Tang[b,c], Fei Mo[a], Xingwang Li[b,c], Erin E. West[a], Daniel Gromer[a,d,4], Jian-Xin Lin[a], Chengyu Liu[e], Yijun Ruan[b,c], and Warren J. Leonard[a,2]

[a]Laboratory of Molecular Immunology and Immunology Center, National Heart, Lung, and Blood Institute, National Institutes of Health (NIH), Bethesda, MD 20892; [b]The Jackson Laboratory for Genomic Medicine, University of Connecticut, Farmington, CT 06030; [c]Department of Genetic and Development Biology, University of Connecticut, Farmington, CT 06030; [d]Medical Research Scholars Program, NIH, Bethesda, MD 20892; and [e]Transgenic Core, National Heart, Lung, and Blood Institute, NIH, Bethesda, MD 20892

This contribution is part of the special series of Inaugural Articles by members of the National Academy of Sciences elected in 2015.

Contributed by Warren J. Leonard, September 27, 2017 (sent for review August 9, 2017; reviewed by Anjana Rao and Ellen V. Rothenberg)

Cytokines critically control immune responses, but how regulatory programs are altered to allow T cells to differentially respond to distinct cytokine stimuli remains poorly understood. Here, we have globally analyzed enhancer elements bound by IL-2–activated STAT5 and IL-21–activated STAT3 in T cells and identified *Il2ra* as the top-ranked gene regulated by an IL-2–activated STAT5-bound superenhancer and one of the top genes regulated by STAT3-bound superenhancers. Moreover, we found that STAT5 binding was rapidly superenriched at genes highly induced by IL-2 and that IL-2–activated STAT5 binding induces new and augmented chromatin interactions within superenhancer-containing genes. Based on chromatin interaction analysis by paired-end tag (ChIA-PET) sequencing data, we used CRISPR-Cas9 gene editing to target three of the STAT5 binding sites within the *Il2ra* superenhancer in mice. Each mutation decreased STAT5 binding and altered IL-2–induced *Il2ra* gene expression, revealing that individual elements within the superenhancer were not functionally redundant and that all were required for normal gene expression. Thus, we demonstrate cooperative utilization of superenhancer elements to optimize gene expression and show that STAT5 mediates IL-2–induced chromatin looping at superenhancers to preferentially regulate highly inducible genes, thereby providing new insights into the mechanisms underlying cytokine-dependent superenhancer function.

superenhancer | STAT5 | ChIA-PET | *Il2ra* gene | IL-2

Superenhancers, also known as stretch enhancers or clustered enhancers, are regulatory elements that typically span more than 10 kb of genomic DNA, are densely bound by transcriptional coactivators, and are associated with high levels of the active chromatin mark histone H3 lysine 27 acetylation (H3K27Ac) (1–4). Superenhancers critically control expression of a subset of genes, including cell type-specific genes that define cell identity (1, 3), and they are often enclosed by CTCF-defined chromatin boundaries that insulate them from neighboring regions. Superenhancers have been described in many cell types (3), but knowledge is limited regarding superenhancer function and how individual enhancer components contribute to gene expression in vivo. Here, we have investigated cytokine-regulated, STAT-dependent superenhancers in the immune system.

After antigen encounter, $CD4^+$ T cells are activated, undergo clonal expansion, and secrete cytokines, including IL-2 and IL-21, which regulate immune differentiation and effector functions. Together with IL-4, IL-7, IL-9, and IL-15, IL-2 and IL-21 share the common cytokine receptor γ chain (5, 6), which is mutated in humans with X-linked severe combined immunodeficiency (7). These cytokines both activate JAK1 and JAK3 (8, 9) but exhibit differential STAT protein utilization (primarily STAT5A and STAT5B for IL-2 and STAT3 for IL-21) (10–13) and, correspondingly, differential gene expression in activated $CD4^+$ T cells. Understanding how regulatory elements within T cells are affected and potentially altered by these cytokines to control distinct gene expression programs is of considerable interest.

Here, we demonstrate that IL-2 and IL-21 rapidly induce the binding of STAT5 and STAT3, respectively, at superenhancer loci. We identified the gene encoding the IL-2 receptor α chain (IL-2Rα) as the top-ranked STAT5-occupied superenhancer locus in mouse T cells, as well as being highly ranked among STAT3-occupied superenhancers. Moreover, STAT5-bound superenhancers were preferentially found in the genes most highly induced by IL-2. Furthermore, using CRISPR-Cas9 technology, we mutated several

Significance

Superenhancers regulate the expression of genes that specify cell type-specific development, but little is known regarding their function and regulation in vivo. Here, we study the cytokines IL-2 and IL-21, which critically control the immune response. These cytokines induce the binding of transcription factors STAT5 and STAT3, respectively, at superenhancers in a cytokine- and gene-specific manner. STAT5-bound superenhancers regulate genes highly induced by IL-2, with STAT5 mediating chromatin looping within such genes, including *Il2ra*, which mediates responsiveness to IL-2. By deleting three STAT5 binding sites that mediate IL-2–induced chromatin looping at the *Il2ra* locus, we demonstrate that superenhancer elements cooperatively control gene expression. Overall, we elucidate cytokine-dependent superenhancer function in general and provide detailed analysis of the *Il2ra* superenhancer.

Author contributions: P.L., S.M., R.S., J.O., W.L., C.L., Y.R., and W.J.L. designed research; P.L., S.M., R.S., J.O., W.L., Z.T., F.M., X.L., E.E.W., D.G., J.-X.L., C.L., and Y.R. performed research; P.L., S.M., R.S., J.O., W.L., Z.T., X.L., C.L., and W.J.L. analyzed data; and P.L., S.M., R.S., J.O., W.L., J.-X.L., and W.J.L. wrote the paper.

Reviewers: A.R., La Jolla Institute and University of California, San Diego; and E.V.R., California Institute of Technology.

Conflict of interest statement: S.M. is now employed by AstraZeneca.

Data deposition: The sequence reported in this paper has been deposited in the GEO database (accession no. GSE102317).

[1]P.L., S.M., R.S., and J.O. contributed equally to this work.

[2]To whom correspondence may be addressed. Email: lip3@nhbli.nih.gov or wjl@helix.nih.gov.

[3]Present address: Respiratory, Inflammatory, and Autoimmune Diseases, Innovative Medicines and Early Development Biotech Unit, AstraZeneca, 43183 Gothenburg, Sweden.

[4]Present address: Perelman School of Medicine, University of Pennsylvania, Philadelphia, PA 19104.

This article contains supporting information online at www.pnas.org/lookup/suppl/doi:10.1073/pnas.1714019114/-/DCSupplemental.

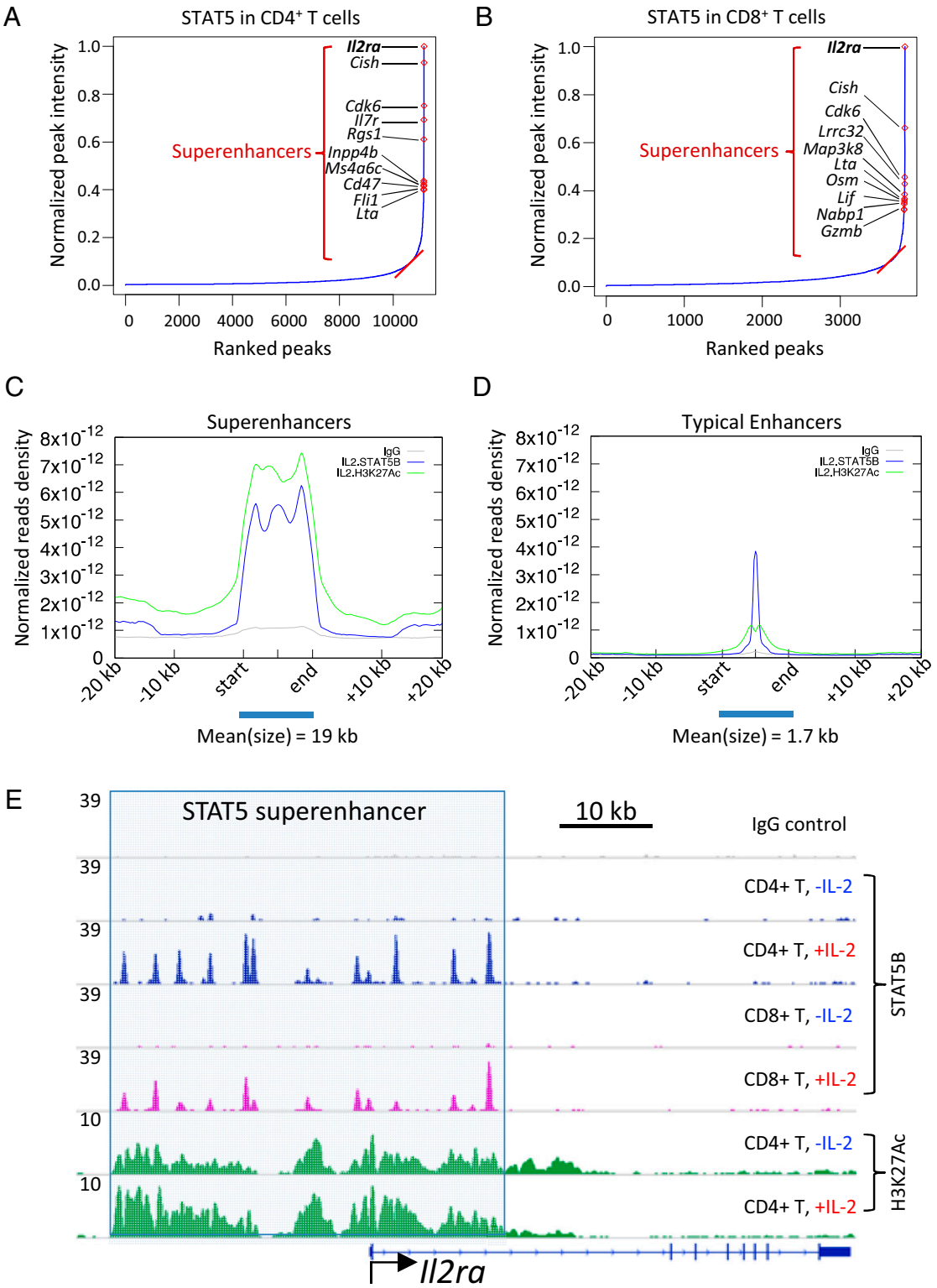

Fig. 1. Identification of genes with STAT5-bound superenhancers. Superenhancer analysis using IL-2–activated STAT5 in preactivated CD4$^+$ T cells (*A*) and preactivated CD8$^+$ T cells (*B*) is illustrated. The *y* axis refers to the normalized density (superenhancer score) of STAT5 binding, whereas the *x* axis represents the ranking of peaks from lowest to highest superenhancer score. Only protein-coding genes were used and plotted in this analysis. Genome-wide profiling analysis using STAT5 and histone H3K27Ac indicates a highly active chromatin status around superenhancer regions (*C*), whereas typical enhancers often span a smaller genomic region and are associated with much lower levels of STAT5 and histone H3K27Ac (*D*). (*E*) STAT5-bound superenhancer at the *Il2ra* locus in CD4$^+$ and CD8$^+$ T cells not stimulated or stimulated with IL-2, based on ChIP-Seq data. Also shown is H3K27Ac in CD4$^+$ T cells not stimulated or stimulated with IL-2.

elements in the *Il2ra* gene in vivo and show that cooperative binding is required to optimize gene expression, thus elucidating the basis for IL-2–mediated superenhancer function.

Results

Identification of STAT5- and STAT3-Bound Superenhancers in T Cells. To investigate how IL-2 and IL-21 activate target genes and the extent to which superenhancers are involved in this process, we first used IL-2–activated STAT5 and IL-21–activated STAT3 to perform a superenhancer analysis (3) in mouse T cells that were preactivated with anti-CD3 plus anti-CD28. We identified 12,792 clustered STAT5 regions, 695 of which scored as superenhancers (Fig. 1*A*) versus 369 of 4,707 clustered STAT3 regions (Fig. S1*A*). Interestingly, upon cytokine stimulation, STAT5- and STAT3-bound superenhancers partially overlapped, but these STAT proteins also were associated with distinct gene loci (compare Fig. 1*A* and Fig. S1*A*). The top-enriched three loci for STAT5 (*Il2ra*, *Cish*, and *Cdk6*) in $CD4^+$ T cells (Fig. 1*A*) were shared in $CD8^+$ T cells (Fig. 1*B*), but there was then divergence, indicating that STAT enrichment at superenhancers partially depends on context. Based on our genome-wide analysis of chromatin immunoprecipitation coupled to DNA sequencing (ChIP-Seq) profiles, we observed that STAT5-enriched superenhancers spanned large genomic regions (average size of ∼19 kb) and indeed were associated with high levels of H3K27Ac (Fig. 1*C*), indicative of highly active chromatin; in contrast, STAT5-dependent typical enhancers (average size of ∼1.7 kb) had much lower density of STAT5 binding and H3K27Ac (Fig. 1*D*). IL-2 is known to potently induce *Il2ra* expression (14) in a STAT5-dependent manner (15–17), and *Il2ra* was, in fact, the gene with the top-ranked superenhancer in preactivated $CD4^+$ and $CD8^+$ T cells based on STAT5 binding (Fig. 1 *A* and *B*). In T cell receptor (TCR) preactivated cells, before IL-2 stimulation, substantial H3K27Ac was evident in the superenhancer region, indicating that the chromatin was already "active" and these preactivated cells were primed to respond to IL-2. Stimulation with IL-2 tended to modestly increase H327Ac within the superenhancer region but, interestingly, to decrease it immediately 3′ of the region (Fig. 1*E*).

STAT5-Bound Superenhancers Preferentially Regulate Genes Highly Induced by IL-2. To determine whether genes with STAT5-bound superenhancers were regulated by IL-2, we next performed RNA-Seq analysis using preactivated $CD4^+$ T cells that were not treated or treated with IL-2 or IL-21 for 0.5, 2, 4, or 24 h. Indeed, IL-2 more potently regulated genes with STAT5-bound superenhancers than genes with STAT5-bound typical enhancers, with effects on gene expression observed within 2 h of IL-2 treatment (Fig. 2 *A* and *B*). Specifically, IL-2 differentially regulated 61, 716, 1,283, and 2,091 genes at 0.5, 2, 4, and 24 h, respectively (Fig. 2*A* and Dataset S1), whereas IL-21 had a more modest effect, regulating 60, 544, 429, and 508 genes, respectively, at the same time points (Fig. S1*B* and Dataset S2). Strikingly, genes highly induced by IL-2 (e.g., *Lta*, *Cish*, *Il2ra*, *Cdk6*) (Fig. 2*B*, Fig. S1*C*, and Dataset S1) or IL-21 (e.g., *Socs3*, *Junb*, *Tha1*, *Il10*) (Fig. S1*D* and Dataset S2) were among the top 10 STAT5- or STAT3-bound superenhancers, and their gene induction was detected within 2 h. We ranked genes with superenhancers based on STAT5 binding intensity into 10 groups and found that the top 10% of STAT5-bound genes were the most inducible (Fig. 2 *C* and *D*; group 1), with induction levels significantly higher than genes with more modest levels of STAT5 binding (Fig. 2*D*; group 2) ($P < 0.0003$), and that the overall expression of genes with superenhancers was significantly higher than those with typical enhancers at each time point evaluated (Fig. 2*E*). STAT5 and STAT3 are closely related proteins and recognize similar γ-IFN–activated sequence (GAS) motifs ($TTCN_3GAA$) (13), and STAT3 tends to have greater ability to bind to noncanonical GAS motifs (18). Analysis of ChIP-Seq data revealed that STAT5 and STAT3 had 18,239 versus 6,397 binding sites, respectively, including both common and distinct binding sites, with a total of 3,773 sites shared by STAT5 and STAT3 (Fig. S1*E*). Among genes with STAT-bound superenhancers, 149 genes bound both IL-2–activated STAT5 and IL-21–activated STAT3 (Fig. S1*F*). Thus, not only are STAT5 and STAT3 differentially activated by IL-2 versus IL-21, but they bind to partially distinct sets of superenhancers and regulate gene expression in a cytokine- and context-specific manner.

Complex Looping Interactions Within the *Il2ra* Gene. Superenhancers are an area of very active investigation (19–23), but knowledge remains limited regarding the roles of superenhancer elements in vivo, whether superenhancers are simply clusters of individual enhancers or instead operate as cooperative functional units, and how/whether elements in superenhancers physically and functionally cooperate to regulate gene expression. As noted above, STAT5 and H3K27Ac are highly enriched at a subset of superenhancers, including at the *Il2ra* superenhancer (Fig. 1 *A*, *B*, and *E*), correlating with IL-2–induced gene expression (Fig. 2*B* and Fig. S1*C*). We also found extensive H3K27Ac and STAT5 binding at the human *IL2RA* locus (Fig. S2), analogous to the mouse *Il2ra* superenhancer, with significant conservation of some of the enhancer elements (Fig. S2).

To clarify how distal enhancer elements within superenhancer loci form enhancer-promoter loops and chromatin interactions, we performed RNA Pol II-based chromatin interaction analysis by paired-end tag (ChIA-PET) sequencing (24, 25) using mouse $CD4^+$ T cells that were preactivated by TCR stimulation (anti-CD3 plus anti-CD28) and then not treated or treated with IL-2 for 4 h. We initially focused primarily on the *Il2ra* gene and integrated together ChIP-Seq data for CTCF, STAT5B, H3K27Ac, and histone H3 lysine 4 trimethylation (H3K4me3) (circos plots in Fig. 3 *A* and *B* and outer four layers and linear plot in Fig. 3*C*) and ChIA-PET RNA Pol II interactions (lines in the inner circle in Fig. 3 *A* and *B* and RNA Pol II peak and loop in Fig. 3*C*). We identified RNA Pol II-mediated chromatin interactions (chromatin looping) in the TCR preactivated control cells (Fig. 3 *A* and *C*), but these interactions were more complex and markedly enhanced following IL-2–induced activation and binding of STAT5 (Fig. 3 *B* and *C*). Strikingly, most of the interaction anchors of IL-2–induced RNA Pol II chromatin interactions overlapped with the induced STAT5 binding sites, indicating that IL-2–activated STAT5 may influence or mediate these chromatin interactions. Interestingly, both H3K4me3 (blue peaks in Fig. 3, primarily at the promoter) and H3K27Ac (green peaks in Fig. 3, spanning the *Il2ra* superenhancer region; also shown in Fig. 1*E*) were strong after TCR preactivation and only modestly affected by stimulation with IL-2, in marked contrast to the changes in STAT5 binding and chromatin looping. We also observed increased IL-2–induced RNA Pol II-based chromatin interactions at the *Cish* (Fig. S3 *A* and *B*) and *Cdk6* (Fig. S3 *C* and *D*) loci, which contain the second and third most highly ranked superenhancers (Fig. 1*A*), as well as at the *Socs1* gene (Fig. S3 *E* and *F*), which, like *Cish*, is an IL-2–induced negative regulator of JAK-STAT5 signaling (26). At the *Il2ra*, *Cish*, *Cdk6*, and *Socs1* loci, most of the STAT5 binding sites overlapped with ends of loop structures identified by ChIA-PET (Fig. 3*C* and Fig. S4), suggesting that the genomic interactions involved were due to or mediated by STAT5 (Fig. 3 and Figs. S3 and S4).

CRISPR-Cas9–Mediated Deletion of STAT5-Bound Elements Diminishes *Il2ra* Superenhancer Activity and Gene Expression. The ChIA-PET analysis revealed chromatin interactions, including those between the promoter and superenhancer regions, but it remained unclear to what extent superenhancers represent a sum of individual enhancers versus an assembly of cooperative components that collectively form a single functional unit to potently enhance gene transcription. We therefore performed genome editing using the CRISPR-Cas9 system (27) to delete STAT5-binding GAS motifs within the *Il2ra* superenhancer corresponding to an upstream

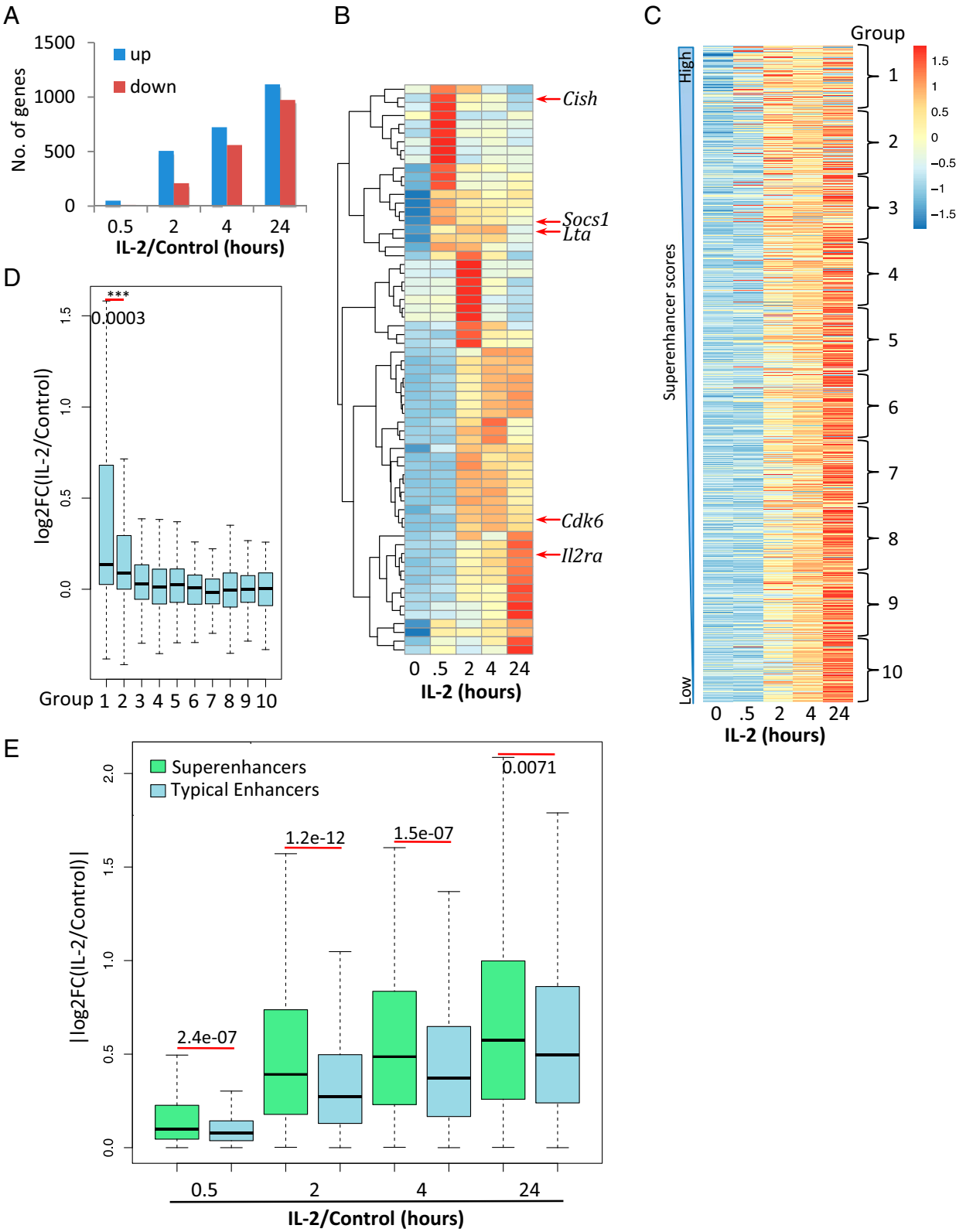

Fig. 2. Genes with STAT5-bound superenhancers are among the most highly IL-2–inducible genes. (*A* and *B*) RNA-Seq analysis of IL-2–regulated gene expression in preactivated $CD4^+$ T cells. (*A*) IL-2 regulates 61, 716, 1,283, and 2,091 genes at 0.5, 2, 4, and 24 h, respectively. (*B*) Heat map showing STAT5-bound superenhancers can be regulated by IL-2 at as early as 0.5 h. (*C*) Heat map of expression profiles of IL-2–regulated genes (sorted by superenhancer binding scores for STAT5, from strongest to weakest) reveals STAT5-bound superenhancer-containing genes (group 1) were highly induced by IL-2. (*D*) Bar graph showing that expression of genes with STAT5-bound superenhancers (group 1) was significantly higher than expression of genes with lower STAT5 binding (group 2) at 0.5 h upon IL-2 stimulation ($P < 0.0003$). Groups 3–10 had even lower STAT5 binding. (*E*) Expression levels of superenhancer-bound genes and typical enhancer-bound genes shown for IL-2 versus control at 0.5, 2, 4, and 24 h.

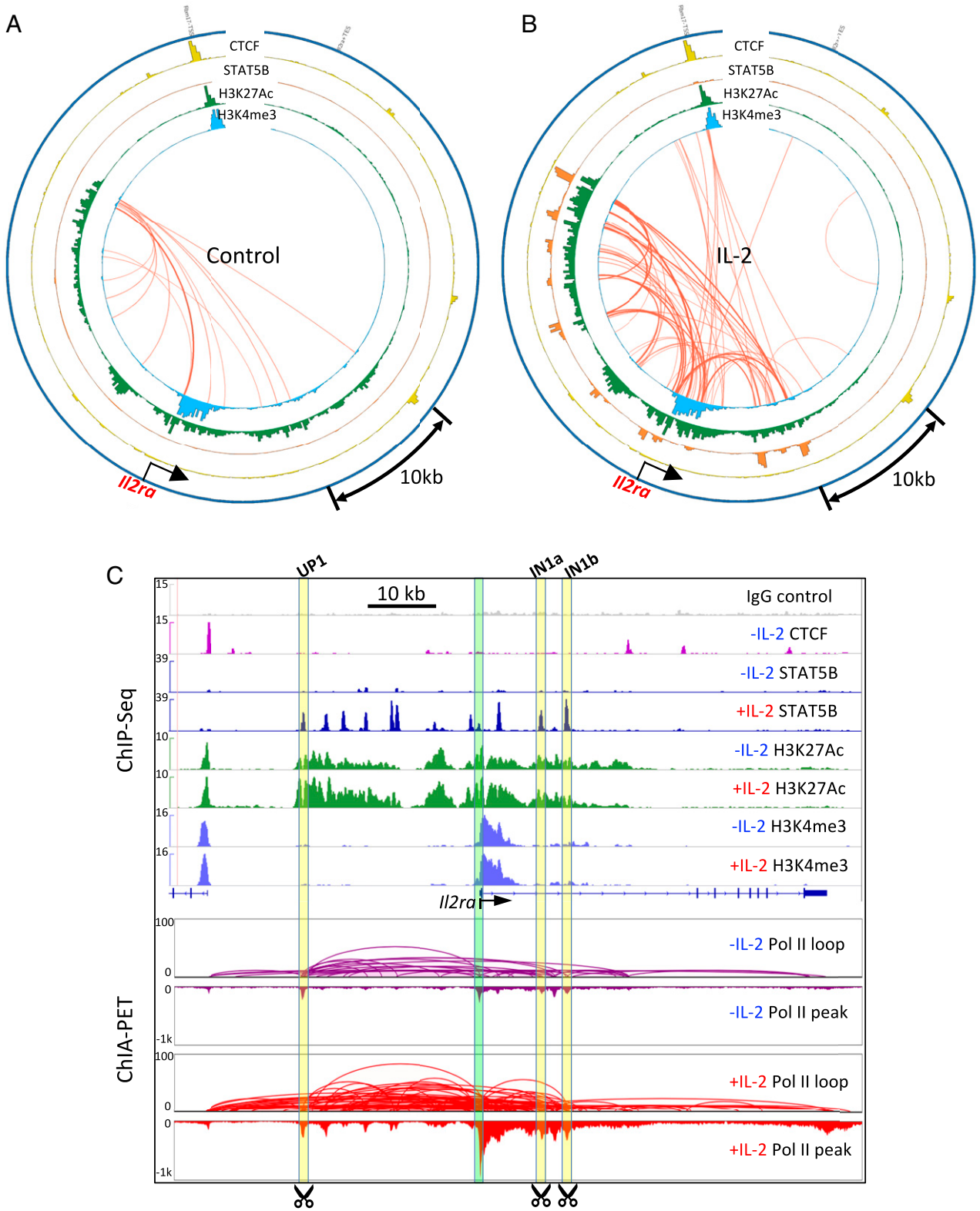

Fig. 3. ChIA-PET and ChIP-Seq analyses reveal complex looping interactions within the *Il2ra* superenhancer. Circos plots show ChIP-Seq data for STAT5, CTCF, H3K27Ac, and H3K4me3 (outer layers) and RNA Pol II-based interactions (connections within inner circles) in control (*A*) and IL-2–treated (*B*) cells. The 5′ → 3′ direction is counterclockwise. CTCF is shown as the potential boundary or insulator of superenhancer regions. Stronger RNA Pol II interaction intensities are indicated by darker red lines. (*C*) Browser view of *Il2ra* genomic locus, with tracks of IgG, CTCF, STAT5, H3K27Ac, and H3K4me3 profiles and RNA Pol II-mediated chromatin interactions without or with IL-2 stimulation. The STAT5 and H3K27Ac (third through sixth tracks) are replicated from Fig. 1*E*. In ChIA-PET loop tracks, the height of the arc denotes the intensity of RNA Pol II-mediated chromatin interaction. Three STAT5 binding (GAS) motifs (UP1, IN1a, and IN1b) within the *Il2ra* superenhancer were deleted using CRISPR-Cas9 (also Fig. S5; deletions are indicated as ΔUP1, ΔIN1a, and ΔIN1b). The *Il2ra* promoter is highlighted with the light green bar, and the three STAT5 binding sites that were targeted by CRISPR-Cas9 are highlighted with yellow bars. Scale bars are indicated in *A* and *B* by the black arcs with double arrows or in *C* by the black line.

element (denoted UP1) and two elements in the first intron (denoted IN1a and IN1b) that strongly bound STAT5, with each of these elements having looping interactions by ChIA-PET (Fig. 3*C*; UP1, IN1a, and IN1b are shown in the yellow boxed regions). Following their targeting by CRISPR-Cas9, we confirmed deletion of the elements (denoted ΔUP1, ΔIN1a, and ΔIN1b) by DNA sequencing (Fig. S5) and then performed ChIP-Seq experiments using anti-STAT5B and preactivated $CD4^+$ T cells from WT and mutant mice to confirm that STAT5 binding was markedly lower at the appropriate positions in the ΔUP1, ΔIN1a, and ΔIN1b mutant mice (Fig. 4*A*), with little, if any, effect on other binding sites. Correspondingly, the activities of WT *Il2ra* luciferase reporter constructs were potently induced by IL-2, but expression was diminished when the corresponding UP1, IN1a, and IN1b sites were mutated (Fig. 4*B*). We next sought to investigate the functional significance of deleting these sites in vivo, using $CD8^+$ T cells to minimize the effects of endogenous IL-2 production by $CD4^+$ T cells. We first purified and treated WT naive $CD8^+$ T cells with 0, 2.5, 25, or 250 nM IL-2, and found that *Il2ra* expression was induced at all time points and at each concentration of IL-2 (Fig. S6*A*). We selected the intermediate dose, 25 nM, for further experiments and found that T cells from ΔIN1a and ΔIN1b mutant mice, compared with cells from littermate control WT mice, were consistently defective in IL-2–induced *Il2ra* expression at all time points evaluated. Of note, the ΔUP1 mutant exhibited higher *Il2ra* expression at day 1, but by day 4, expression was significantly lower than was observed in the control mice (Fig. 4*C*). We also measured IL-2Rα (CD25) protein expression in WT and mutant $CD8^+$ T cells stimulated with IL-2. At days 1 and 2, the ΔUP1 T cells tended to have higher IL-2Rα expression, but by day 4, all mutants, including ΔUP1, had significantly lower IL-2Rα expression than observed with WT T cells (Fig. 4*D* and Fig. S6*B*). These data reveal that the *Il2ra* superenhancer is not simply composed of a group of independent and potentially redundant enhancers but rather comprises a set of regulatory elements that cooperatively mediate normal expression.

Discussion

In this study, we have investigated superenhancers induced by IL-2–STAT5 and IL-21–STAT3. The gene encoding IL-2Rα in T cells was potently induced, a finding consistent with the well-established IL-2–mediated induction of *IL2RA* (28–30) and *Il2ra* (17), in part, via STAT5 tetramers (17) and with the defective IL-2–induced *Il2ra* expression in both $Stat5a^{-/-}$ (16) and $Stat5b^{-/-}$ (15) mice. Somewhat unexpectedly, it was also highly responsive to IL-21–STAT3, but this is consistent with defective IL-2–induced *Il2ra* gene induction in $Stat3^{-/-}$ T cells (31).

We used ChIA-PET analysis to define dynamic chromatin interactions within superenhancer loci. Although IL-2 caused only modest changes in H3K27Ac, it robustly augmented both STAT5 binding and looping structures in multiple genes that were highly induced by IL-2, including *Il2ra*, underscoring the utility of ChIA-PET to identify dynamic changes in chromatin structure. Because IL-2–activated STAT5 may influence or mediate chromatin interactions, it will be interesting to investigate whether these interactions at the *Il2ra* gene are altered or eliminated in situations of *Stat5* deficiency or in STAT5 tetramer-deficient double–knock-in mice (17). In addition, the effects of the deletions on long-range chromatin interactions is another area for future investigation.

Analysis of CRISPR-mediated deletions of three elements in the *Il2ra* superenhancer revealed that individual regulatory elements were not functionally redundant, given partial loss of activity when any of these elements was deleted. Moreover, T cells from WT mice had much higher *Il2ra* expression than cells from any of the mutant mouse lines, indicating the importance of the overall integrity of the STAT5 superenhancer for sustaining normal IL-2Rα expression. Deletion of individual enhancer elements can have cell type-specific effects. For example, a 3′ enhancer in the *Il4* gene regulates cytokine production by Th2 cells and mast cells, via differential regulation of CNS-2 and HS4 elements (32), and a distal conserved sequence element can control *Ifng* gene expression by T cells and natural killer cells (33). Thus, more in-depth experiments are required to analyze the consequences and cell type-specific effects of these mutants in vivo.

Our data also reveal that STAT5 superenhancers in T cells are preferentially associated with genes that are highly induced by IL-2. In preactivated cells, H3K27Ac and H3K4me3 marks are already present, but it is IL-2 stimulation that potently induces not only STAT5 binding but also chromatin looping that is anchored at these binding sites, thus providing new insights into the roles and mechanisms underlying gene regulation controlled by STAT5 and cytokine-dependent superenhancers. In addition to identifying the mouse *Il2ra* superenhancer, we confirmed an analogous area of extensive STAT5 binding at the human *IL2RA* locus. It is possible that naturally occurring mutations in these superenhancer elements might diminish IL-2Rα expression, with an impact on the immune response and potential susceptibility to diseases.

Materials and Methods

Mice. Six- to 8-wk-old C57BL/6 mice were used as WT controls. CRISPR-Cas9–targeted mice were generated by the transgenic core of the National Heart, Lung, and Blood Institute (NHLBI). All experiments were performed under protocols approved by the NHLBI Animal Care and Use Committees and followed NIH guidelines for use of animals in intramural research.

Generation of CRISPR-Cas9 Mutant Mice. To delete the GAS motifs at the UP1 [−25.7 kb from *Il2ra* transcription start site (TSS)], IN1a (+10.8 kb from *Il2ra* TSS), and IN1b (+12.5 kb from *Il2ra* TSS) sites, we designed two CRISPR single-guide RNAs (sgRNAs) for each site using MIT's CRISPR online tool (crispr.mit.edu/). The specific sgRNA sequences are indicated in Fig. S5. The selected sgRNA sequences (CTGTCATCTGAGGGTTTCGA and TGAGAAGTGTGTGACTCAAA for UP1, TTGAAATGCTATCAGATGCA and GCTAGCAACCGGCAAAACAG for IN1a, and ATTACAACTTGCTTCTCAGA and AGAAGCAAGTTGTAATCGTG for IN1b) were individually cloned into an sgRNA vector using OriGene's sgRNA cloning services. Then, sgRNAs were in vitro-transcribed using the MEGAshortscript T7 kit (Life Technologies). Cas9 mRNA was in vitro-synthesized from the MLM3613 plasmid vector (no. 42251; Addgene) using the mMESSAGE mMACHINE T7 kit (Life Technologies). For deleting each GAS motif, two sgRNAs (50 ng/μL each sgRNA) were mixed with Cas9 mRNA (100 ng/μL) and then coinjected into the cytoplasm of fertilized mouse eggs. After culturing overnight in M16 medium (EMD Millipore), those embryos that reached the two-cell stage of development were implanted into the oviducts of pseudopregnant foster mothers. Mice born to these foster mothers were genotyped by PCR amplification of the targeted regions, followed by DNA sequencing.

Isolation of Cells and Cell Culture. T cells were isolated by standard methods using kits from Miltenyi Biotec. Cells were cultured in RPMI 1640 medium containing 10% FBS. For preactivation, cells were stimulated with plate-bound anti-CD3 (2 μg/mL) plus anti-CD28 (1 μg/mL) for 3 d, rested overnight, and then stimulated with IL-2 (100 U/mL, 2 nM) or IL-21 (100 ng/mL).

Reporter Assays. $CD8^+$ T cells were activated for 24 h with anti-CD3 plus anti-CD28 and washed, and 10^7 cells were electroporated with 10 μg of reporter plasmid (pGL4.23[luc2/minP]; Promega), containing WT or mutant constructs cloned 5′ of the minimal promoter, and 2 μg of pRL-TK (Promega) in 0.4 mL of RPMI 1640 medium using settings of 960 μF and 250 V. The constructs were generated as follows: the 905-bp UP1 WT and 884-bp UP1 deletion fragments and the 955-bp IN1b WT and 943-bp IN1b deletion fragments were each cloned between the KpnI and HindIII sites, whereas the 900-bp IN1a WT and 814-bp IN1a deletion fragments were each cloned between the XhoI and HindIII sites in pGL4.23. Schematic diagrams of the reporter plasmids are shown in Fig. 4*B*, and DNA sequences and primers are described in Dataset S3. Cells were immediately stimulated with IL-2. Dual-luciferase assays were performed 16 h later (Promega). Luciferase activity was determined relative to the control pRL-TK activity.

ChIP-Seq and RNA-Seq Library Preparation and Sequencing. ChIP-Seq experiments were performed as previously described (17, 34, 35). RNA-Seq experiments were performed as previously described with total RNA isolated

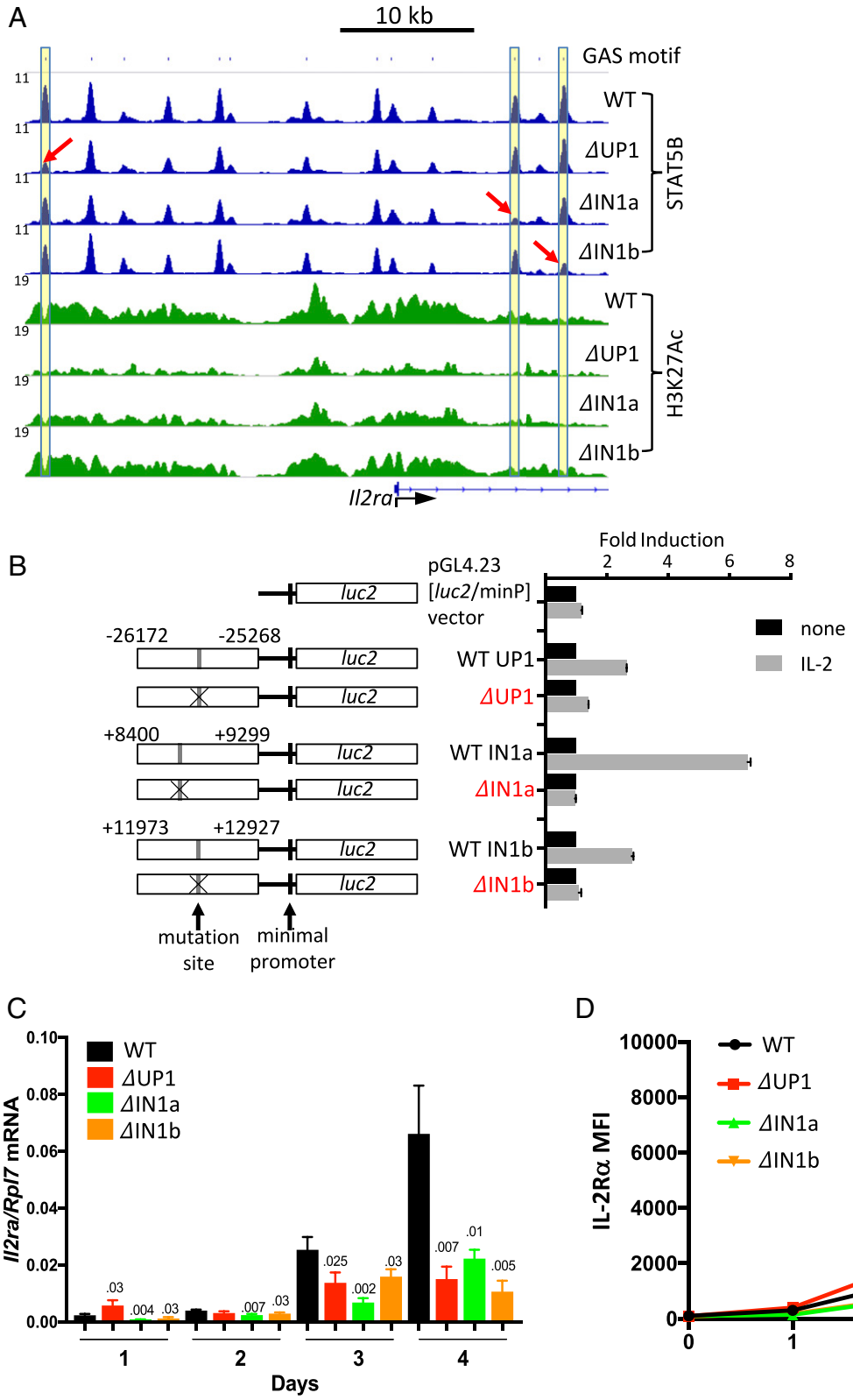

Fig. 4. CRISPR-Cas9 deletions of STAT5-bound elements and functional impact on *Il2ra* superenhancer activity and gene expression. (*A*) ChIP-Seq analysis of STAT5 binding in preactivated CD4$^+$ T cells in WT, ΔUP1, ΔIN1a, and ΔIN1b mutant mice, with targeted sites highlighted in yellow and with red arrows pointing to decreased STAT5 binding at corresponding sites. (*B*) Luciferase assays in cells expressing WT or ΔIN1a, ΔIN1b, and ΔUP1 mutant *Il2ra* reporter constructs. Constructs (*Left*) were transfected into preactivated CD8$^+$ T cells and treated without or with IL-2 for 16 h (*Right*; $n = 3$, mean ± SD). Dataset S3 shows the sequences for the WT and mutant reporter constructs. (*C*) *Il2ra* mRNA induction in T cells from WT versus ΔIN1a, ΔIN1b, and ΔUP1 mutant mice in response to 25 nM IL-2 at indicated time points. (*D*) IL-2Rα protein expression in T cells from the indicated mice stimulated with IL-2 for 1, 2, 3, and 4 d. Shown are data from the combination of two experiments, with a total of five animals.

from mouse $CD4^+$ T cells, preactivated, and treated without or with IL-2 or IL-21 for 0.5, 2, 4, or 24 h.

ChIP-Seq and RNA-Seq Analysis. PCR products were bar-coded (indexed) and sequenced on Illumina Genome Analyzer II and HiSeq2000 platforms. Sequenced reads (25 bp or 50 bp, single end, depending on the platforms) were obtained with the Illumina CASAVA pipeline and mapped to the mouse genome mm9 (National Center for Biotechnology Information build 37, July 2007) using Bowtie 1.0.1. Only uniquely mapped reads were retained. The mapped outputs were converted to browser-extensible data files, which were then converted to binary tiled data files (TDFs) using IGVTools 2.3.32 for viewing on the Integrative Genomics Viewer browser (36) (software.broadinstitute.org/software/igv/home). TDFs represent the average alignment or feature density for a specified window size across the genome. For ChIP-Seq data, we mapped reads into nonoverlapping 20-bp windows for transcription factors STAT3 and STAT5 and histone modifications H3K4me3 and H3K27Ac. The reads were shifted 100 bp from their 5′ starts to represent the center of the DNA fragment associated with the reads. For RNA-Seq data, raw counts that fell on exons of each gene were calculated and normalized by using reads per kilobase per million mapped reads. Differentially expressed genes were identified with the R Bioconductor package "edgeR" (37), and the expression heat maps were generated with the R package "pheatmap."

Peak Calling and Superenhancer Analysis. MACS 1.4.2 (38) was used to call binding sites (peaks) relative to control libraries. The probability value threshold was set as 1×10^{-5}, and the effective genome size was set as 1.87×10^9 bp. Only nonredundant reads were analyzed for peak calling. The superenhancer discovery approach was based on STAT5 or STAT3 occupancy but, otherwise, was analogous to the original strategy used by Whyte et al. (3) and was performed using HOMER (39) with the following settings: -style super -o auto -superSlope -1,000 -minDist 15,000. Superenhancers were identified as regions with "slope" (focus ratio)/(region size annotation enhancer) greater than 1. Only protein-coding genes were retained for further analysis.

RNA Pol II ChIA-PET Analysis, Library Construction, and Sequencing. RNA Pol II-based ChIA-PET was performed as previously described (24, 25, 40). Briefly, ~100–200 million cells were harvested and fixed with 30 mL of 1.5 mM ethylene glycol bis[succinimidylsuccinate] in PBS buffer for 45 min at room temperature. To cross-link the cells, formaldehyde was added to a final concentration of 1% for 20 min at room temperature and then neutralized with 0.125 M glycine. Cells were lysed using cell lysis buffer and nuclear lysis buffer. Chromatin was obtained and sonicated to generate fragments with an average length of 300 bp. The anti-RNA Pol II monoclonal antibody 8WG16 (MMS-126R; Covance) was used to enrich RNA Pol II-bound chromatin fragments. ChIP DNA on beads was used for ChIA-PET library preparation. After performing end repair and A-tailing using T4 DNA polymerase (New England Biolabs) and the Klenow enzyme, the ChIP DNA ends were proximity-ligated by the single-biotinylated bridge linker (forward strand: 5′-[5Phos]CGCGATATC/iBIOdT/TATCTGACT-3′, reverse strand: 5′-[5Phos]GTCAGATAAGATATCGCGT-3′), with the 3′ nucleotide T overhanging on both strands. Proximity ligation DNA was reverse cross-linked and fragmented, and sequencing adaptors were added simultaneously by using Tn5 transposase (Nextera kit; Illumina). DNA fragments containing the bridge linker at ligation junctions were captured by streptavidin beads and used as templates for PCR amplification. These DNA products were then subjected to size-selection and paired-end sequencing (2×150 bp) using an Illumina HiSeq2500 sequencer.

RNA Pol II ChIA-PET Data Processing. The ChIA-PET data were processed by a customized ChIA-PET v2 data processing pipeline, as described (40). Briefly, the bridge linker was scanned in each PET sequence, and only the PETs with bridge linkers were used for downstream analysis. After trimming the bridge linkers, the sequences flanking the linker were mapped to the mouse reference genome mm9 using bwa-mem with default parameter settings. Only the uniquely aligned PETs with a mapping quality of greater than 30 were retained. PCR duplicates were removed using the MarkDuplicates tool of the Picard Tools library. Each PET was categorized as either a self-ligation PET (two ends of the same DNA fragment) or interligation PET (two ends from two different DNA fragments in the same chromatin complex), depending on the genomic span between the two ends of a PET or origin of the two ends of a PET from two different chromosomes. PETs with both ends originating from the same chromosome and a genomic span less than 8 kb were classified as self-ligation PETs. Self-ligation PETs were used as a proxy for ChIP fragments since they were derived in a manner analogous to ChIP-Seq mapping for protein binding sites. PETs with both ends originating from the same chromosome and a genomic span of greater than 8 kb were classified as interligation PETs. PETs with each end from a different chromosome were also classified as interligation PETs. The interligation PETs reflect the long-range chromatin interaction mediated by proteins of interest. To accurately represent the frequency of interaction between two loci, both ends of interligation PETs were extended by 500 bp along the reference genome and PETs overlapping at both ends (with extension) were grouped as a single PET cluster. Individual interligation PETs that could not be merged as PET clusters were referred to as singletons. A singleton is similar to Hi-C data in a function to reflect high-order chromatin topology (40). All uniquely mapped and nonredundant reads, including self-ligation and interligation PETs, were used to calculate the RNA Pol II binding coverage along the chromosomes for visualization. For all of these reads, to identify binding peaks, we used MACS 1.4.2 (38) with default parameters.

ACKNOWLEDGMENTS. This work was supported by the Division of Intramural Research and Transgenic Core at the NHLBI and the Jackson Laboratory for Genomic Medicine.

1. Hnisz D, et al. (2013) Super-enhancers in the control of cell identity and disease. *Cell* 155:934–947.
2. Pott S, Lieb JD (2015) What are super-enhancers? *Nat Genet* 47:8–12.
3. Whyte WA, et al. (2013) Master transcription factors and mediator establish super-enhancers at key cell identity genes. *Cell* 153:307–319.
4. Parker SC, et al.; NISC Comparative Sequencing Program; National Institutes of Health Intramural Sequencing Center Comparative Sequencing Program Authors; NISC Comparative Sequencing Program Authors (2013) Chromatin stretch enhancer states drive cell-specific gene regulation and harbor human disease risk variants. *Proc Natl Acad Sci USA* 110:17921–17926.
5. Leonard WJ, Noguchi M, Russell SM, McBride OW (1994) The molecular basis of X-linked severe combined immunodeficiency: The role of the interleukin-2 receptor gamma chain as a common gamma chain, gamma c. *Immunol Rev* 138:61–86.
6. Leonard WJ (1996) The molecular basis of X-linked severe combined immunodeficiency: Defective cytokine receptor signaling. *Annu Rev Med* 47:229–239.
7. Noguchi M, et al. (1993) Interleukin-2 receptor gamma chain mutation results in X-linked severe combined immunodeficiency in humans. *Cell* 73:147–157.
8. Miyazaki T, et al. (1994) Functional activation of Jak1 and Jak3 by selective association with IL-2 receptor subunits. *Science* 266:1045–1047.
9. Russell SM, et al. (1994) Interaction of IL-2R beta and gamma c chains with Jak1 and Jak3: Implications for XSCID and XCID. *Science* 266:1042–1045.
10. Leonard WJ, Spolski R (2005) Interleukin-21: A modulator of lymphoid proliferation, apoptosis and differentiation. *Nat Rev Immunol* 5:688–698.
11. Liao W, Lin JX, Leonard WJ (2011) IL-2 family cytokines: New insights into the complex roles of IL-2 as a broad regulator of T helper cell differentiation. *Curr Opin Immunol* 23:598–604.
12. Rochman Y, Spolski R, Leonard WJ (2009) New insights into the regulation of T cells by gamma(c) family cytokines. *Nat Rev Immunol* 9:480–490.
13. Leonard WJ, O'Shea JJ (1998) Jaks and STATs: Biological implications. *Annu Rev Immunol* 16:293–322.
14. Kim HP, Kelly J, Leonard WJ (2001) The basis for IL-2-induced IL-2 receptor alpha chain gene regulation: Importance of two widely separated IL-2 response elements. *Immunity* 15:159–172.
15. Imada K, et al. (1998) Stat5b is essential for natural killer cell-mediated proliferation and cytolytic activity. *J Exp Med* 188:2067–2074.
16. Nakajima H, et al. (1997) An indirect effect of Stat5a in IL-2-induced proliferation: A critical role for Stat5a in IL-2-mediated IL-2 receptor alpha chain induction. *Immunity* 7:691–701.
17. Lin JX, et al. (2012) Critical Role of STAT5 transcription factor tetramerization for cytokine responses and normal immune function. *Immunity* 36:586–599.
18. Kwon H, et al. (2009) Analysis of interleukin-21-induced Prdm1 gene regulation reveals functional cooperation of STAT3 and IRF4 transcription factors. *Immunity* 31:941–952.
19. Adam RC, et al. (2015) Pioneer factors govern super-enhancer dynamics in stem cell plasticity and lineage choice. *Nature* 521:366–370.
20. Hay D, et al. (2016) Genetic dissection of the α-globin super-enhancer in vivo. *Nat Genet* 48:895–903.
21. Kitagawa Y, et al. (2017) Guidance of regulatory T cell development by Satb1-dependent super-enhancer establishment. *Nat Immunol* 18:173–183.
22. Shin HY, et al. (2016) Hierarchy within the mammary STAT5-driven Wap super-enhancer. *Nat Genet* 48:904–911.
23. Vahedi G, et al. (2015) Super-enhancers delineate disease-associated regulatory nodes in T cells. *Nature* 520:558–562.
24. Fullwood MJ, et al. (2009) An oestrogen-receptor-alpha-bound human chromatin interactome. *Nature* 462:58–64.
25. Li G, et al. (2012) Extensive promoter-centered chromatin interactions provide a topological basis for transcription regulation. *Cell* 148:84–98.

26. Sporri B, Kovanen PE, Sasaki A, Yoshimura A, Leonard WJ (2001) JAB/SOCS1/SSI-1 is an interleukin-2-induced inhibitor of IL-2 signaling. *Blood* 97:221–226.
27. Jinek M, et al. (2012) A programmable dual-RNA-guided DNA endonuclease in adaptive bacterial immunity. *Science* 337:816–821.
28. John S, Robbins CM, Leonard WJ (1996) An IL-2 response element in the human IL-2 receptor alpha chain promoter is a composite element that binds Stat5, Elf-1, HMG-I(Y) and a GATA family protein. *EMBO J* 15:5627–5635.
29. Lécine P, et al. (1996) Elf-1 and Stat5 bind to a critical element in a new enhancer of the human interleukin-2 receptor alpha gene. *Mol Cell Biol* 16:6829–6840.
30. John S, Vinkemeier U, Soldaini E, Darnell JE, Jr, Leonard WJ (1999) The significance of tetramerization in promoter recruitment by Stat5. *Mol Cell Biol* 19: 1910–1918.
31. Akaishi H, et al. (1998) Defective IL-2-mediated IL-2 receptor alpha chain expression in Stat3-deficient T lymphocytes. *Int Immunol* 10:1747–1751.
32. Solymar DC, Agarwal S, Bassing CH, Alt FW, Rao A (2002) A 3′ enhancer in the IL-4 gene regulates cytokine production by Th2 cells and mast cells. *Immunity* 17: 41–50.
33. Hatton RD, et al. (2006) A distal conserved sequence element controls Ifng gene expression by T cells and NK cells. *Immunity* 25:717–729.
34. Li P, et al. (2012) BATF-JUN is critical for IRF4-mediated transcription in T cells. *Nature* 490:543–546.
35. Liao W, Lin JX, Wang L, Li P, Leonard WJ (2011) Modulation of cytokine receptors by IL-2 broadly regulates differentiation into helper T cell lineages. *Nat Immunol* 12: 551–559.
36. Robinson JT, et al. (2011) Integrative genomics viewer. *Nat Biotechnol* 29:24–26.
37. Robinson MD, McCarthy DJ, Smyth GK (2010) edgeR: A Bioconductor package for differential expression analysis of digital gene expression data. *Bioinformatics* 26: 139–140.
38. Zhang Y, et al. (2008) Model-based analysis of ChIP-Seq (MACS). *Genome Biol* 9:R137.
39. Heinz S, et al. (2010) Simple combinations of lineage-determining transcription factors prime cis-regulatory elements required for macrophage and B cell identities. *Mol Cell* 38:576–589.
40. Tang Z, et al. (2015) CTCF-mediated human 3D genome architecture reveals chromatin topology for transcription. *Cell* 163:1611–1627.